Journal of the Korean Electrochemical Society
Vol. 4, No. 1, 2001, 21-25

총 설

Application of Fractal Geometry to Interfacial Electrochemistry - I. Diffusion Kinetics at Fractal Electrodes

Heon-Cheol Shin and Su-Il Pyun†

Corrosion and Interfacial Electrochemistry Research Laboratory at Department of Materials Science and Engineering, Korea Advanced Institute of Science and Technology, 373-1 Kusong-Dong, Yusong-Gu, Taejon 305-701, KOREA
(Received February 1, 2001 : Accepted February 21, 2001)

Abstract : This article is concerned with the application of the fractal geometry to interfacial electrochemistry. Especially, we dealt with diffusion kinetics at the fractal electrodes. This article first explained the basic concepts of the fractal geometry which has proven to be fruitful for modelling rough and irregular surfaces. Finally this article examined the electrochemical responses to various signals under diffusion-limited reactions during diffusion towards the fractal interfaces: The generalised forms, including the fractal dimension of the electrode surfaces, of Cottrell, Sand and Randles-Sevcik equations were theoretically derived and explained in chronoamperomety, chronopotentiometry and linear sweep/cyclic voltammetry, respectively.

초 록 : 프랙탈 기하학의 계면 전기화학에로의 응용과 관련하여 프랙탈 표면을 향한 이온/원자 확산의 속도론에 대하여 다루었다. 우선 프랙탈 기하학의 기본 개념에 대하여 설명하였고, 이를 바탕으로 이온/원자의 확산 현상과 관련하여 다양한 전기적 입력하에서 전극 표면의 프랙탈 특성에 기인하는 특수한 반응 양상이 설명되었다. Chronoamperometry, chronopotentiometry 및 linear sweep/cyclic voltammetry 실험시에 각각 관찰되는, 전극의 프랙탈 차원이 포함된 일반화된 Cottrell, Sand 및 Randles-Sevcik 관계를 이론적으로 유도하였고, 그 의미에 대하여 설명하였다.

Key words : Fractal, Rough electrode, Generalised Cottrell equation, Generalised Sand equation, Generalised Randle-Sevcik equation

1. Introduction

The power law, *e.g.* Cottrell, Sand or Randles-Sevcik relation, of the electrochemical diffusion of an active species from a bulk electrolyte towards an electrode surface was introduced a long time ago under the assumption of geometrically simple (*e.g.* planar, cylindrical or spherical) electrode,[1] and it has been frequently used to analyse transport phenomena in the field of electrochemistry. However, the geometrical assumption is not justified if the electrode surface is irregular. Such cases occur frequently in practice, because the actual solid electrode can be rough, porous, and partially blocked, *etc*. That is, the conventional power laws place a limitation to describe the electrochemical atomic/ionic diffusion towards rough or irregular electrode, due to the complicated and non-uniform current density distribution on the electrode surface.

Recently, following the Mandelbrot's pioneering work[2] on the fractal geometry, much attention has been paid to the modelling of the rough and irregular surfaces as fractal.[3-7] And many theoreticians have focussed on finding some correlation between the modelled(assumed) fractal electrode geometry and certain electrochemical quantity.[8-20] These efforts have been quite successful and thus the anomalous diffusion behaviour in the rough electrode has been satisfactorily analysed on grounds of the fractal geometry.

This article reviewed the basic concepts of the fractal geometry. In addition, we examined the electrochemical responses to various signals under diffusion-limited reactions during diffusion towards the fractal interfaces: We theoretically derived the generalised forms, including the fractal dimension of the electrode surface, of Cottrell, Sand and Randles-Sevcik equations.

2. Fundamentals of Fractals

2.1. Concepts of fractals and fractal dimension

Mandelbrot defined a fractal to be any curve or surface that is independent of scale.[2] This property, referred to as self-similarity, means that any portion of curve, if blown up in scale, would appear identical to the whole curve. An important difference between the fractal curves and the idealised curves that are normally applied to natural processes is that fractals are nowhere differentiable. That is, although they are continuous, they are kinked everywhere.

For example, let us imagine a straight line of length l, as in Fig. 1(a). One then removes the middle third of the line, and replaces with two lines that each has the same length $(1/3)l$ as the remaining lines on each side (Fig. 1(b)). Consequently, the length of the curve becomes $(4/3)l$. The above process specifies a rule that is used to generate a new form. The rule says to take each line and replace it with four lines,

†E-mail: sipyun@mail.kaist.ac.kr

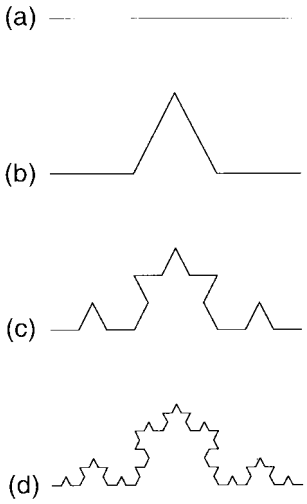

Fig. 1. The first few stages in the construction of the von Koch curve. One removes the middle third of a straight line (a), and replaces with two lines that each has the same length as the remaining lines on each side, resulting in (b). Application of this procedure to each of the line segments leads to curve (c), and then to curve (d). This process can be repeated ad infinitum.

the length of which becomes one-third of the original. Thus, the second iteration according to the rule yields a more convoluted curve as shown in Fig. 1(c), which consists of 4^2 straight lines. The length of curve becomes $(4/3)^2 l$. And subsequent third iteration gives the curve (Fig. 1(d)) with 4^3 lines of length $(1/3)^3 l$, thus with a total length $(4/3)^3 l$. Iterating this process n times leads to a curve with 4^n lines of length $(1/3)^n l$, thus with a total length $(4/3)^n l$. One does this process without end, resulting in a mathematical "monstrosity" : A continuous curve of infinite length which is nowhere differentiable. Moreover, if blown up in scale, any portion of the curve appears identical to the whole curve, *i.e.* the curve is self-similar.

Now let us consider the dimension of the von Koch curve. So far we have used the term "dimension" in two senses : The three dimension of Euclidean space, and the number of variables in a dynamic system. More formally and generally, we say a set is n-dimensional if we need n independent variables to describe a neighborhood of any point. If we take an object with a measure (*e.g.* length, area or volume) of N residing in Euclidean(or topological) dimension D_E, and reduce its linear size by $1/m$ in each spatial direction, it is well known that its measure would increase to be $N' = m^{D_E}N$. We will call this a simple magnification. Here, D_E has the values of one, two and three for line, plane and solids such as cube, respectively. Fig. 2(b) shows the product of simple magnification (m=3) of Fig. 2(a). The magnified curve can not be the von Koch curve any more, because it loses already the self-similarity.

The fractal character of the von Koch curve can survive not through the simple magnification, but through the fractal magnification (Fig. 2(c)). In the case of the fractal magnification, the length of the three times magnified line becomes always the four times of that length of the original line, so that from the relation $4 = 3^D1$ we find the dimension $D=(ln$ 4)/(ln 3) ≅ 1.2619. The dimension between 1 and 2 indicates that the von Koch curve has properties intermediate between those of one- and two-dimension objects. This fractional dimension can not be explained by the conventional Euclidean concept. One calls the fractional dimension of the fractal objects the fractal or Hausdorff dimension D_H. If the horizontal cross section of the complete electrode is given as the von Koch curve mentioned above, the fractal dimension of this electrode becomes D_H=1+(ln 4)/(ln 3) ≅ 2.2619.

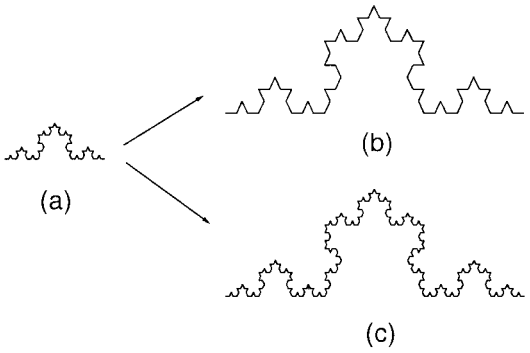

Fig. 2. The simple magnification of the image (a) yields (b), while the fractal magnification of the image (a) yields (c).

2.2. Inner and outer cut-offs

Real objects obviously do not show the fractal behaviour at length zero to infinity. For example, metal fractures are only extremely crinkly (down to the limits of their microstructural size range), while fractals are infinitely crinkly. Hence, it can not be said that every real objects are ideally fractals. Nevertheless, real bodies and surfaces can be modelled by fractals in a certain limited size of range bordered by spatial cut-offs, *i.e.* inner cut-off λ_i and outer cut-off λ_o.

So far as the diffusion process is concerned, spatial cut-offs (λ_i and λ_o), and the corresponding temporal break-times (τ_i and τ_o) are connected by $\delta \approx \sqrt{2\tilde{D}t}$ (where, δ is the root mean square displacement of the diffusion species, *i.e.* the diffusion layer width, $\tilde{D}$ is the chemical diffusivity, and t represents the time).[21] Beyond the temporal break-time τ_i or τ_o when the diffusion species hardly recognise the fractal character of the surface, the electrochemical responses to various signals obey the conventional diffusion equations, while between τ_i and τ_o, the corresponding equations are expressed as their generalised forms including the fractal dimension of the surface. Here, one has to keep in mind that at short times ($t \ll \tau_i$) and long times ($t \gg \tau_o$) the surface area stands for the microscopic area A_{micr} and macroscopic area A_{macr}, respectively.

3. Diffusion towards Fractal Surfaces

3.1. Potentiostatic technique; Chronoamperometry; Curent transient method

Consider an inert metal with a fractal surface immersed into an electrolyte containing a redox couple. We assume that the diffusion of the oxidised species *Ox* and the reduced

species *Red* in the electrolyte is semi-infinite. For the sake of simplicity we assume further the solution contains initially (at $t = 0$) only the oxidised form and the bulk and surface concentrations are identical, *i.e.* $c_{ox}^{b} = c_{ox}^{s}$. The electrode is held initially at a potential where no electrode reaction takes place. The only reaction occurring when the potential is lowered, is the reversible reduction of the oxidised species *Ox* to the reduced species *Red* by $Ox + ze = Red$.

Now, we are interested in the time dependence of the Faradaic current when a potential step is applied.[10,14] Assume that the effective D_H prevails between the inner cutoff λ_i and the outer cutoff λ_o. And then enlarge the interface by a factor m as described in the preceding Section. In the simple magnification (Fig. 2(b)), every point of the original system in the bulk or at the interface can be mapped onto the enlarged one as $\vec{r} \rightarrow m\vec{r}$, where $\vec{r}$ is a position vector in a suitably chosen coordinate system. And the concentration map $c_{simple}(m\vec{r}, t') = c(\vec{r}, t)$ holds provided that the time is scaled appropriately. For this, the structure of the diffusion equation and the boundary conditions require $t'=m^2t$. The total current is obtained from Fig. 2(b) as the flux multiplied by the area. Since the flux is proportional to the concentration gradient at the surface, it scales m^{-1}. And the area is proportional to m^2. Then we obtain the conventional following scaling law for the current

$$i_{simple}(m, m^2t) = mi(1, t) \tag{1}$$

, where the first argument refers to system size.

In the fractal magnification (Fig. 2(c)), as long as the root mean square displacement of the diffusing particles is smaller compared with the outer cutoff λ_o, local properties dominate and the large scale structure has very little effect on the diffusion current. Therefore, since for Fig. 2(c) area scales as m^{D_H}, we obtain

$$i_{fractal}(m, t) = m^{D_H} i(1, t) \tag{2}.$$

Now in case that the root mean square displacement of the diffusing particles is larger than λ_i where the effect of the smallest irregularities disappears, we have the approximate equality $i_{simple}(m, t) = i_{fractal}(m, t)$. Consequently, from the combination of Eqs. (1) and (2), we get

$$i(m, m^2t)/i(m, t) = m^{1-D_H} \tag{3}$$

, which has the following solution

$$i = \sigma \cdot t^{-\alpha_D},\ \alpha_D = (D_H - 1)/2 \tag{4}$$

, where σ means the Cottrell coefficient. The power-law behaviour represented by Eq. (4) is valid both between the temporal cutoffs τ_i and τ_o corresponding to the spatial cutoffs λ_i and λ_o (see Section 2.2), and outside the temporal cutoffs.

Let us consider the Cottrell coefficient σ. Outside the cutoffs, the conventional Cottrell equation $i = \sigma_c t^{-1/2}$ holds where σ_c has the form[1]

$$\sigma_c = \frac{zFAc_{ox}^{b}\sqrt{\tilde{D}_{ox}}}{\pi^{1/2}} \tag{5}.$$

In Eq. (5) the area A has to be specified. As explained in Section 2.2, the diffusing species sees the microscopic area A_{micr} for $t \ll \tau_i$ and the macroscopic area A_{macr} for $t \gg \tau_o$. Pajkossy and Nyikos defined the temporal cutoffs τ_i and τ_o as $\gamma \cdot \lambda_i^2/\tilde{D}_{ox}$ and $\gamma \cdot \lambda_o^2/\tilde{D}_{ox}$, respectively.[14] Here, γ means a dimensionless geometrical factor. We can now find the generalised Cottrell coefficient σ_g for the diffusion towards the fractal surfaces. For obvious continuity reason we can give the following equations at the temporal cutoffs.

$$\sigma_g t^{-(D_H-1)/2} = \frac{zFA_{micr}c_{ox}^{b}\sqrt{\tilde{D}_{ox}}}{\pi^{1/2}} t^{-1/2} \text{ at } t = \gamma\lambda_i^2/\tilde{D}_{ox} \tag{6}$$

$$\sigma_g t^{-(D_H-1)/2} = \frac{zFA_{macr}c_{ox}^{b}\sqrt{\tilde{D}_{ox}}}{\pi^{1/2}} t^{-1/2} \text{ at } t = \gamma\lambda_o^2/\tilde{D}_{ox} \tag{7}$$

Thus, from Eqs. (6) and (7), we get the generalised Cottrell coefficient σ_g :

$$\sigma_g = \frac{zFA_{micr}c_{ox}^{b}\sqrt{\tilde{D}_{ox}}}{\pi^{1/2}}\left[\frac{\gamma\lambda_o^2}{\tilde{D}_{ox}}\right]^{D_H/2-1} = \frac{zFA_{macr}c_{ox}^{b}\sqrt{\tilde{D}_{ox}}}{\pi^{1/2}}\left[\frac{\gamma\lambda_i^2}{\tilde{D}_{ox}}\right]^{D_H/2-1} \tag{8}.$$

Since either A_{macr} and λ_o, or A_{micr} and λ_i can be measured for a given surface, and the reasonable value of γ is known to be $1/\pi$,[14] we can quantitatively analyse diffusion towards the fractal interfaces during the potential step experiment using the following generalised Cottrell equation

$$i = \sigma_g t^{-(D_H-1)/2} \tag{9}.$$

Another important mathematical works on the problem of diffusion towards the fractal interfaces have been performed recently with the help of fractional calculus.[18] Those works have proposed the following generalised diffusion equation involving a fractional derivative operator.

$$\frac{\partial^{(3-D_H)}c}{\partial t^{(3-D_H)}} = \tilde{D}_{ox}^{*}\frac{\partial^2 c}{\partial x^2} \tag{10}$$

, where $\tilde{D}_{ox}^{*}$ is the fractional diffusivity defined as $K^{(4-2D_H)} R_o^{(2D_H-4)} \tilde{D}_{ox}^{(3-D_H)}$ (K is a constant related to the fractal dimension and R_o is the side length of a square electrode), and $\partial^\nu/\partial t^\nu$ means the Riemann-Liouville mathematical operator of fractional derivative :

$$\frac{\partial^\nu c}{\partial t^\nu} = \frac{1}{\Gamma(1-\nu)}\frac{d}{dt}\int_0^t \frac{c(\xi)}{(t-\xi)^\nu} d\xi \tag{11}.$$

During the potential step experiment, the initial condition (I.C.) and the boundary condition (B.C.) are given as

$$\text{I.C. : } c = c_{ox}^{b} \text{ for } 0 \le x < \infty \text{ at } t = 0 \tag{12}$$

$$\text{B.C. : } c = c_{ox}^{b} \text{ for } x \rightarrow \infty \quad \text{(semi-infinite constraint) at } t \ge 0 \tag{13}$$

$$c = 0 \quad \text{for } x = 0 \quad \text{(potentiostatic constraint) at } t > 0 \tag{14}.$$

Using the Laplace transforms of Eqs. (10), (12)-(14), then we get

$$\bar{c}_{ox}(x, s) = \frac{c_{ox}^b}{s}\left[1 - \exp\left(-\sqrt{\frac{s^{3-D_H}}{\tilde{D}_{ox}^*}}x\right)\right] \quad (15)$$

, where s is the Laplace variable.

To compute the time dependence of the current density, we make use of the following relation

$$i(t) = -zF\tilde{D}_{ox}^*\left(\frac{\partial c_{ox}}{\partial x}\right)_{x=0} \quad (16).$$

From the combination of the Laplace transform of Eq. (16) and the derivative of Eq. (15) at x=0, we get

$$\bar{i}(s) = zF\sqrt{\tilde{D}_{ox}^*}c_{ox}^b\sqrt{s^{D_H-3}} \quad (17).$$

Finally the inverse Laplace transform of Eq. (17) yields

$$i(t) = \frac{zF\sqrt{\tilde{D}_{ox}^*}c_{ox}^b}{\Gamma\left(\frac{3-D_H}{2}\right)}t^{-\frac{D_H-1}{2}} \quad (18)$$

, which is a generalised Cottrell equation. The Cottrell equation for planar diffusion is retrieved for $D_H = 2$.

3.2. Galvanostatic technique; Chronopotentiometry; Potential transient method

Consider that a constant current density i is applied at the electrode/electrolyte interface. Then, the diffusing species begins to be depleted at the interface. At a certain characteristic time τ, called the transition time, the concentration drops to zero at the interface. The relation between the transition time and the fractal dimension of the electrode surface has been explored also using fractional calculus. The I.C. of Eq. (12) and B.C. of Eq. (13) are still valid in this case, whereas the B.C. of Eq. (14) is replaced with the following galvanostatic boundary condition at the electrode/electrolyte interface

$$\text{B.C. : } i = -zF\tilde{D}_{ox}^*\left(\frac{\partial c_{ox}}{\partial x}\right) \text{ for } x = 0 \text{ (galvanostatic constraint) at } t > 0 \quad (19).$$

Using the Laplace transform of Eqs. (10),(12),(13) and (19), the following equation is given[18)]

$$\bar{c}_{ox}(x, s) = \frac{c_{ox}^b}{s} - \left(\frac{i}{zF\sqrt{\tilde{D}_{ox}^*}s^{(5-D_H)/2}}\right)\exp\left(-\sqrt{\frac{s^{3-D_H}}{\tilde{D}_{ox}^*}}x\right) \quad (20).$$

The inverse Laplace transform of Eq. (20) yields

$$c_{ox}(x, t) = c_{ox}^b - \frac{i}{zF\tilde{D}_{ox}^*}\left[2\sqrt{\frac{\tilde{D}_{ox}^* t^{3-D_H}}{\pi}}\exp\left(-\frac{x^2}{4\tilde{D}_{ox}^* t^{3-D_H}}\right) - x \cdot erfc\left(\frac{x}{2\sqrt{\tilde{D}_{ox}^* t^{3-D_H}}}\right)\right] \quad (21).$$

At the transition time τ, the concentration of the oxidised species Ox drops to zero at the electrode/electrolyte interface x=0. So the generalised Sand equation is obtained from Eq. (21).

$$\frac{i\tau^{\frac{D_H-1}{2}}}{c_{ox}^b} = zF\sqrt{\tilde{D}_{ox}^*}\Gamma\left(\frac{D_H+1}{2}\right) \quad (22)$$

The Sand equation for planar diffusion is retrieved for $D_H = 2$.

3.3. Linear sweep/cyclic voltammetry

We consider again the redox reaction $Ox + ze = Red$ with a solution initially containing only the oxidised form Ox. The electrode held initially at a potential E_i where no electrode reaction takes place. For the sake of simplicity, it is assumed that the diffusion coefficients of species Ox and Red are equal, *i.e.* $\tilde{D}=\tilde{D}_{ox}=\tilde{D}_{red}$. Now, the potential is linearly increased or decreased with $E(t)=E_i \pm \nu t$ (ν is a potential scan rate, and signs "+" and "–" represent anodic scan and cathodic scan, respectively). Under the assumption that the redox couple is reversible, the surface concentrations c_{ox}^s and c_{red}^s of Ox and Red, respectively, are always determined by the electrode potential through the Nernst equation

$$E = E_{1/2} + \frac{RT}{zF}\ln\left(\frac{c_{ox}^s}{c_{red}^s}\right) \quad (23)$$

, where $E_{1/2}$ means the half-wave potential, *i.e.* the potential bisecting the distance between anodic and cathodic peaks in a cyclic voltammogram.

The relationship between the difference in surface and bulk concentrations and current is known to be[15,22)]

$$\Delta c_{ox} = c_{ox}^s - c_{ox}^b = \int_0^t i(t-\tau)f(\tau)d\tau \quad (24).$$

This may be recognised as a convolution integral which, when Laplace transformed, gives the following relation

$$\Delta\bar{c}_{ox}(s) = \bar{i}_{ox}(s) \cdot \bar{f}_{ox}(s) \quad (25)$$

, where $\bar{f}_{ox}$ is the transfer function for the process of the oxidised species Ox.[22)] $\bar{f}_{ox}$ can be calculated from the potential step experiment : Assuming an extremely fast kinetics at the electrode surface, Δc_{ox} is a step function during the potential step experiment, and thus the Laplace transform $\Delta\bar{c}_{ox}$ is given as $-c_{ox}^b/s$. And since $i_{ox}(t)$ is given by $\sigma_g t^{-(D_H-1)/2}$ (see Section 3.1), we get $\bar{f}_{ox}$ as

$$\bar{f}_{ox}(s) = \frac{\Gamma\left(\frac{1}{2}\right)}{zFA_{macr}\tilde{D}_{ox}^{1/2}\left(\frac{\gamma\lambda_i}{\tilde{D}_{ox}}\right)^{D_H/2-1}\Gamma\left(\frac{3-D_H}{2}\right)}s^{-(D_H-1)/2} \quad (26).$$

Then, substituting Eq. (26) into Eq. (25) and using the inverse Laplace transform, we get[19,20)]

$$c_{ox}^s(t) = c_{ox}^b - \frac{\Gamma\left(\frac{1}{2}\right)}{zFA_{macr}\tilde{D}_{ox}^{1/2}\left(\frac{\gamma\lambda_i^2}{\tilde{D}_{ox}}\right)^{D_H/2-1}\Gamma\left(\frac{3-D_H}{2}\right)}\frac{1}{\Gamma\left(\frac{D_H-1}{2}\right)}\int_0^t\frac{i(\tau)d\tau}{(t-\tau)^{(3-D_H)/2}} \quad (27).$$

Extending the derivation for a perfect smooth two dimensional surface,[1)] we finally obtain the following functional expression for the diffusion-limited current on the fractal interface during cyclic voltammetry.

$$i(t) = \frac{zFA_{macr}\tilde{D}_{ox}^{1/2}\left(\frac{\gamma\lambda_i^2}{\tilde{D}_{ox}}\right)^{D_H/2-1} c_{ox}^{b}\Gamma\left(\frac{3-D_H}{2}\right)\Gamma\left(\frac{D_H-1}{2}\right)}{\Gamma\left(\frac{1}{2}\right)(RT)^{(D_H-1)/2}} \times (zFv)^{(D_H-1)/2}\chi(\sigma t) \quad (28)$$

, where $\sigma t = (zF/RT)vt = (zF/RT)(E_i - E)$. χ is a dimensionless parameter defined as

$$\int_0^{\sigma t}\frac{\chi(z)dz}{(\sigma t - z)^{(D_H-1)/2}} = \frac{1}{1+\theta\cdot S(\sigma t)} \quad (29)$$

, where $\theta = \exp[(zF/RT)(E_i - E_{1/2})]$ and $S(t) = \exp(-\sigma t)$. Now at any given value of $S(\sigma t)$, which is a function of E, $\chi(\sigma t)$ can be obtained by numerical solution of Eq. (29), and thus the current is available by Eq. (28).

It is interesting to note that the conventional Randles-Sevcik equation, relating the peak current i_{peak} to the potential scan rate $v^{1/2}$, does not hold for the fractal electrode case. Instead it is replaced with the following generalised Randles-Sevcik equation, relating i_{peak} to the scan rate $v^{(D_H-1)/2}$.

$$i_{peak} = \frac{zFA_{macr}\tilde{D}_{ox}^{1/2}\left(\frac{\gamma\lambda_i^2}{\tilde{D}_{ox}}\right)^{D_H/2-1} c_{ox}^{b}\Gamma\left(\frac{3-D_H}{2}\right)\Gamma\left(\frac{D_H-1}{2}\right)}{\Gamma\left(\frac{1}{2}\right)(RT)^{(D_H-1)/2}} \times (zFv)^{(D_H-1)/2}\chi_{\max}(\sigma t_{\max}) \quad (30)$$

The Randles-Sevcik equation for planar diffusion is retrieved for D_H=2.

4. Concluding Remarks

The present article presented first the basic concepts of the fractal geometry and then theoretically derived the generalised forms, including the fractal dimension of the electrode surface, of Cottrell, Sand and Randles-Sevcik equations. The usual 0.5 exponent in conventional Cottrell, Sand and Randles-Sevcik equations is replaced with $(D_H - 1)/2$ exponent in the case of the fractal electrode of dimension D_H.

Consequently, the fractal geometry provides an efficient tool to treat problems arising from the irregular geometries of the electrode: The geometrical irregularities can be modelled on the basis of fractals, and then one can describe the abnormal electrochemical behaviour of geometrically irregular electrodes in chronoamperometry, chronopotentiometry and linear sweep/cyclic voltammetry, by considering the diffusion towards the fractal interfaces, especially by using the generalised equations described above.

References

1. A. J. Bard and L. R. Faulkner, “Electrochemical Methods”, 143, 218, 253, John Wiley and Sons, Inc., New York (1980).
2. B. B. Mandelbrot, “The Fractal Geometry of Nature”, 1, Freeman, New York (1983).
3. B. B. Mandelbrot, D. E. Passoja and A. J. Paullay, *Nature*, **308**, 721 (1984).
4. E. E. Underwood and K. Banerji, *Mater. Sci. & Eng.*, **80**, 1 (1986).
5. C. S. Pande, L. E. Richards, N. Louat, B. D. Dempsey and A. J. Schwoeble, *Acta Metall.*, **35**, 1633 (1987).
6. Z. G. Wang, D. L. Chen, X. X. Jiang, S. H. Ai and C. H. Shih, *Scripta Metallurgia*, **22**, 827 (1988).
7. C. W. Lung and S. Z. Zhang, *Physica D*, **38**, 242 (1989).
8. A. Le Mehaute and G. Crepy, *Solid State Ionics*, **9&10**, 17 (1983).
9. L. Nyikos and T. Pajkossy, *Electrochim. Acta*, **30**, 1533 (1985).
10. L. Nyikos and T. Pajkossy, *Electrochim. Acta*, **31**, 1347 (1986).
11. W. H. Mulder and J. H. Sluyters, *Electrochim. Acta*, **33**, 303 (1988).
12. B. Sapoval, J. -N. Chazalviel and J. Peyriere, *Phys. Rev. A*, **38**, 5867 (1988).
13. M. Blunt, *J. Phys. A: Math. Gen.*, **22**, 1179 (1989).
14. T. Pajkossy and L. Nyikos, *Electrochim. Acta*, **34**, 171 (1989).
15. T. Pajkossy and L. Nyikos, *Electrochim. Acta*, **34**, 181 (1989).
16. T. Pajkossy and L. Nyikos, *Phys. Rev. B*, **42**, 709 (1990).
17. T. Pajkossy, A. P. Borosy, A. Imre, S. A. Martemyanov, G. Nagy, R. Schiller and L. Nyikos, *J. Electroanal. Chem.*, **366**, 69 (1994).
18. Y. Dassas and P. Duby, *J. Electrochem. Soc.*, **142**, 4175 (1995).
19. M. Stromme, G. A. Niklasson and C. G. Granqvist, *Phys. Rev. B*, **52**, 14192 (1995).
20. M. Stromme, G. A. Niklasson and C. G. Granqvist, *Solid State Commun.*, **96**, 151 (1995).
21. T. Pajkossy, *J. Electroanal. Chem.*, **300**, 1 (1991).
22. H. E. Keller and W. H. Reinmuth, *Anal. Chem.*, **44**, 434 (1972).